

Oxide and metallic materials for photovoltaic applications: A Review

S. Nivetha^{1, 2}, R. Perumalsamy^{1, 2}, A. Ayeshamariam^{1, 3,*},
A. Mohamed Saleem^{1, 4},
M. Karunanithy^{1, 5}, M. Jayachandran⁶



¹Research and Development Center, Bharathidasan University, Thiruchirappalli, 620 024, India

^{1,2}Department of Physics, Sir Theagaraya Higher Secondary School, Chennai, 600 021, India

^{1, 3*} Department of Physics, Khadir Mohideen College, Adirampattinam, 614 701, India

^{1,4}Department of Physics, Jamal Mohamed College, Thiruchirappalli, 620024, India

^{1,5}Department of Physics, SKPD Boys Higher Secondary School, Chennai, 600 001, India

⁶Department of Physics, Sree Sethu Institute of Technology, Pulloor, Kariapatti, 626 115, India

*) E-mail: aismma786@gmail.com

Received 18/2/2018, Accepted 23/4/2018, Accepted 15/5/2019

Materials and its properties are the main criteria to build its applications; some of the photovoltaic materials could be used in pure form to fabricate photovoltaic applications of the materials LCD (liquid crystal display), LED (Light emitting diodes), photodiodes and photo transistors. When it will be doped with oxide semiconducting materials its applications will be enhanced commercially. The resultant photovoltaic nanocomposites can be easily changed by its shape and parameters. The transparent conductor is applied to the touch screen panel and it is confirmed that all the final devices operate under continuous mechanical stress. This review gave the simple basic ideas of its development from 19 century to recent. The technologies of the photovoltaic applications and its electronic devices were dealt in this review. The unique optical properties of graphene were reported the use of solution processed high quality transparent conductive electrode in an organic solar cell. This review also deals with the reports of many researchers and their fabrications of thieno [3,4-*b*] thiophene/benzodithiophene: phenyl-C₇₁-butyric acid methyl ester (PTB7:PCB₇₁M) bulk heterojunction organic solar cell based on the exfoliated graphene (EG) anode exhibits a power conversion efficiency for next-generation flexible optoelectronic devices.

Keywords: PV materials, Efficiency, Solar cells and amorphous Silicon

1. INTRODUCTION

Solar cells based on compound semiconductors (III–V and II–VI) were first investigated in the 1960s. At the same time, polycrystalline Si (pc-Si) and thin-film solar cell technologies were developed to provide high production capacity at reduced material consumption and energy input during fabrication, allows integration in the structure of modules by deposition, and consequently reduce the cost for large-scale terrestrial applications [1]. According to Shockley and Queisser (1961), the thermodynamic efficiency for an ideal single-junction cell is around 31% [2]. This finding can be attributed to the fact that the efficiency of a single-junction device is limited by the transmission loss of photons with energies below the bandgap and by the thermal relaxation of carriers created by photons with energies above the bandgap [3]. The efficiency of solar cells can be increased by capitalization of the solar spectrum through the use of multi-junction cells that combine two or more cells with different bandgaps. Tandem cells prepared using different materials with different bandgaps can significantly increase the efficiency. Over 41% efficiency has already been achieved from multi-junction cells that are presently being used mainly in space applications [4].

The lab efficiency of commonly used crystalline PV cells has now increased from 6% in the 1950s to over 22%. In terms of composition, PV cells display a wide range of diversity; mono- and poly-crystalline silicon PV cells are now being commercially combined with PV cells prepared from gallium–arsenide, gallium–antimony, copper–indium–diselenide, and cadmium–telluride. While plastic and organic PV cells are still in the research and development phase, multi-junction tandem PV cells with an efficiency of over 40% are already in market. Continuous research and development facilitate the development of efficient and economical solar cells.

(Peumans, P., 2013) [5]. A recent study published in *Nature* has revealed the development of low-cost newly developed PVs at Princeton University. The devices are made from organic materials that consist of small carbon-containing molecules as opposed to the conventional inorganic, silicon-based materials. These PV cells consist of materials that are ultra-thin and flexible and could be applied to large surfaces. The color of the cells can also be varied, making them attractive architectural elements. These cells are not only economical but have also achieved a significant increase in efficiency, from 1% in the first organic solar cell developed in 1986 to nearly 5% in newly developed cells. With further developments, the research is targeting to improve the efficiency of these cells to 10% (REW, 2013) [6], partnership in Germany has reportedly developed organic cells with 12% efficiency.

Clinical technologies cover a broad variety of areas, which include sensors, devices, instrumentation, and modeling. The area is managed under the engineering theme but may link to research areas to the Healthcare technologies theme. High-efficiency white organic light-emitting diodes (OLEDs) (Opto Light Emitted diodes) fabricated on silver nanowire-based composite transparent electrodes show almost perfect Lambertian emission and superior angular color stability, which are imparted by electrode light scattering. The efficiencies of OLEDs are comparable with those fabricated using indium tin oxide (ITO). The transparent electrodes are fully solution processable, thin film compatible, and suitable for large area devices [7].

Metal nanowire transparent networks are promising replacements to ITO transparent electrodes for optoelectronic devices. While transparency and sheet resistance are key metrics for transparent electrode performance, independent control of the film's light scattering properties is important in developing multifunctional electrodes for improved PV absorption. In the present study, we show that the controlled incorporation of ZnO nanopyramids into a metal nanowire network film affords an independent, highly tunable control of the scattering properties (haze) with minimal effects on transparency and sheet resistance. Varying the zinc oxide/silver nanostructure ratios prior to spray deposition results in sheet resistance, transmission (600 nm), and haze (600 nm) of 6–30 $\Omega \text{ cm}^{-1}$, 68–86%, and 34–66%, respectively. Incorporation of zinc oxide nano pyramid scattering agents into the conducting nanowire mesh exerts a negligible effect on mesh connectivity, providing a straightforward method of controlling electrode scattering properties. Decoupling of the film scattering power and electrical characteristics renders these films promising candidates for highly scattering transparent electrodes in optoelectronic devices and can be generalized to other metal nanowire films as well as carbon nanotube transparent electrodes [8].

2. DISCUSSION ABOUT THE VARIETIES OF ORGANIC AND POLYMER SOLAR CELLS

The class of materials combining high electrical or thermal conductivity, optical transparency, and flexibility is crucial for the development of many future electronic and optoelectronic devices. Silver nanowire networks show very promising results and represent a viable alternative to the commonly used, scarce, and brittle ITO [9]. The efficiency of today's most efficient organic solar cells is limited by the ability of the active layer to absorb all the sunlight. While internal quantum efficiencies exceeding 90% are common, the external quantum efficiency rarely exceeds 70%. Light trapping techniques that increase the ability of a given active layer to absorb light are common in inorganic solar cells but have only been applied to organic solar cells with limited success. We analyze the light trapping mechanism for a cell with a V-shape substrate configuration and demonstrate significantly improved photon absorption in 5.3% efficient PCDTBT:PC₇₀ BM bulk heterojunction polymer materials used as a solar cell. The measured short circuit current density improves by 29%, which agrees with model predictions, and the power conversion efficiency increases to 7.2%, a 35% improvement over the performance in the absence of a light trap [10]. All-solid-state donor–acceptor planar-heterojunction (PHJ) hybrid solar cells are constructed, and their excellent performance is measured. The deposition of a thin C₆₀ fullerene or fullerene-derivative (acceptor) layer in vacuum on a CH₃NH₃PbI₃ perovskite (donor) layer creates a hybrid PHJ that displays the PV effect. Such heterojunctions are suitable for the development of efficient newly structured hybrid solar cells [11]. Single exciton fission transforms a molecular singlet excited into two triplet states, each with half the energy of the original singlet. In solar cells, it could potentially double the photocurrent from high-energy photons.

We demonstrate organic solar cells that exploit singlet exciton fission in pentacene to generate more than one electron per incident photon in a portion of the visible spectrum shown in Fig 1(a-b). The use of a fullerene acceptor, a poly (30 hexylthiophene) exciton confinement layer, and a conventional optical trapping scheme generated a peak external quantum efficiency of (109±1)% at wavelength $\lambda = 670 \text{ nm}$ for a 15 nm-thick pentacene film. The corresponding

internal quantum efficiency is $160\% \pm 10\%$. Analysis of the magnetic field effect on photocurrent suggests that the triplet yield approaches 200% for pentacene films thicker than 5 nm [12]. Sukjoon et al.[13] introduced a facile approach to fabricate a metallic grid transparent conductor on a flexible substrate through the selective laser sintering of metal nanoparticle ink. Metallic grid transparent conductors with high transmittance ($>85\%$) and low sheet resistance (30 ohm/sq) are readily produced on glass and polymer substrates at a large scale without any vacuum or high-temperature environment. The resultant metallic grid also shows superior stability in terms of adhesion and bending. The transparent conductor is further applied to the touch screen panel, and results confirm that the final device firmly operates under continuous mechanical stress.

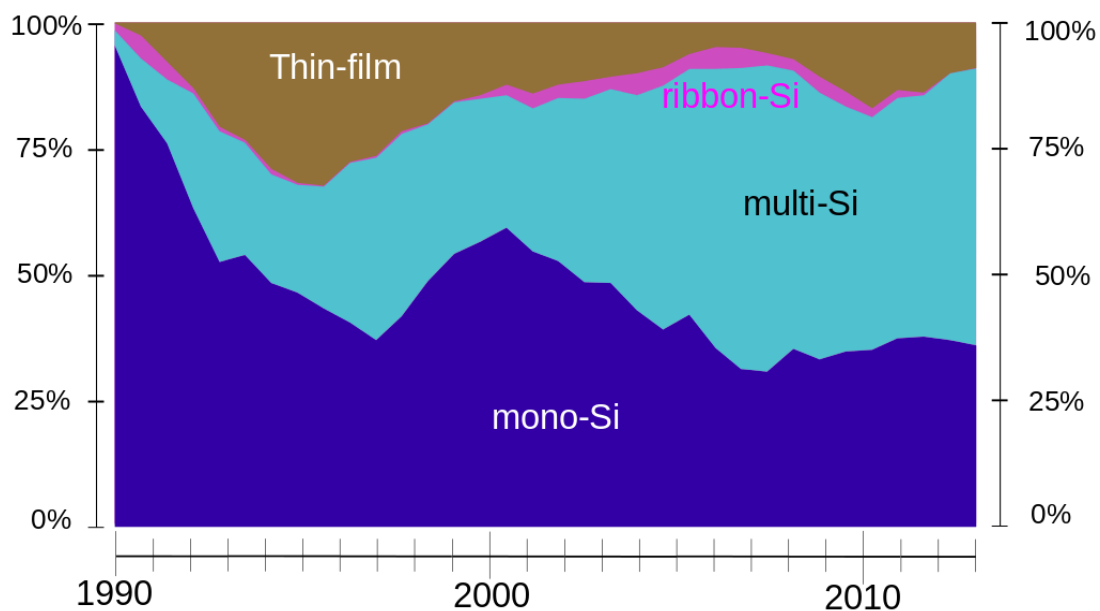


Figure 1a. Evaluation of Global market share by PV Thin Film Technology from 1990 to 2013

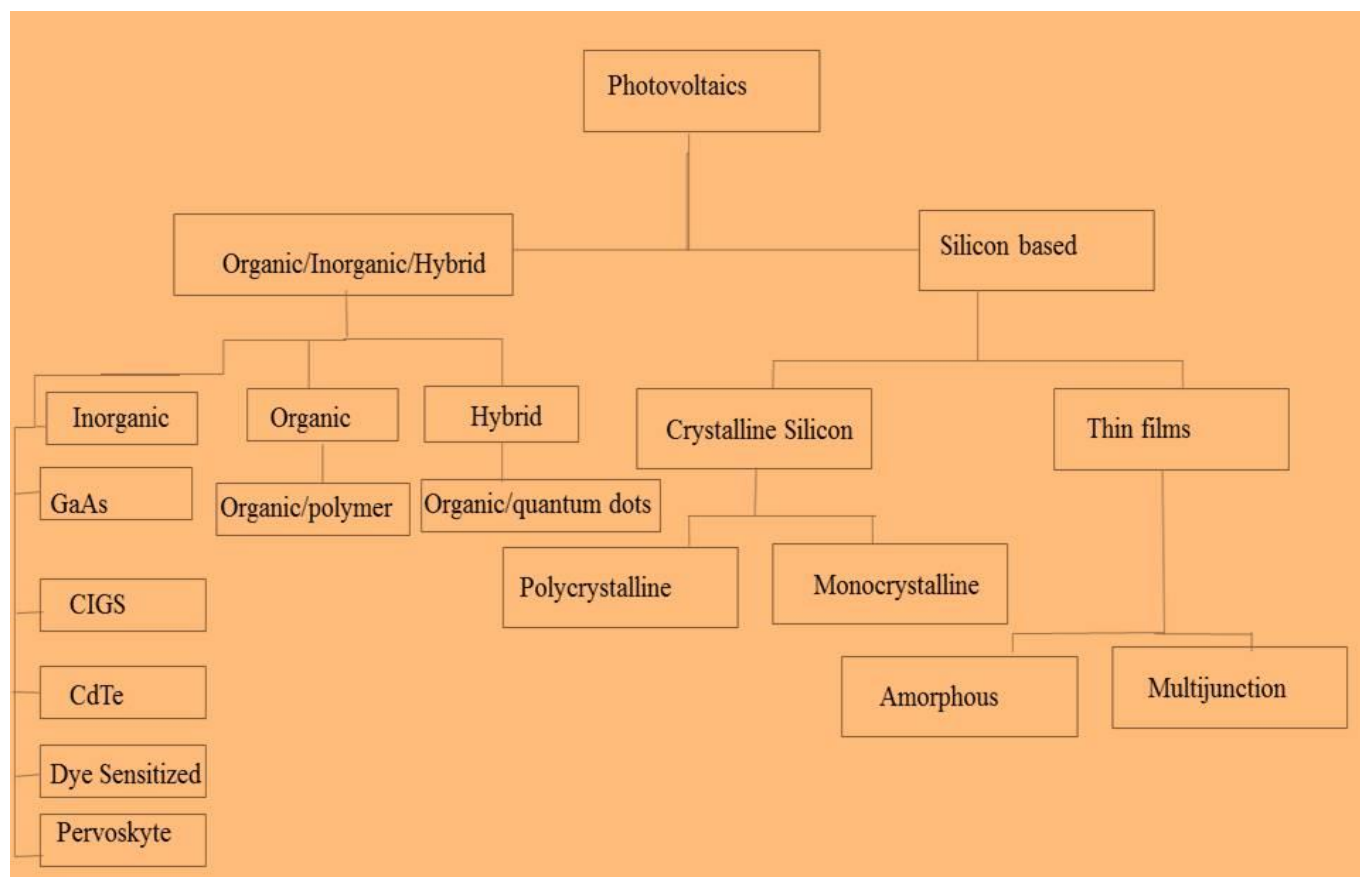


Figure 1 (b) Bock diagram of types of photovoltaic materials and Applications of Single crystalline and multi crystalline Si

2.1 Efficiency of different solar cells

We demonstrate a novel approach to fabricate conductive silver electrodes rapidly on transparent flexible substrates with high bonding strength by direct laser writing. A new type of silver ink composed of silver nitrate, sodium citrate, and poly vinylpyrrolidone (PVP) was prepared in this work. The role of PVP was elucidated to improve the quality of silver electrodes. Silver nanoparticles and sintered microstructures were simultaneously synthesized and patterned on a substrate using a focused 405 nm continuous wave laser. The writing was completed through the transparent flexible substrate with a programmed 2D scanning sample stage. Silver electrodes fabricated by this approach exhibit a remarkable bonding strength, which can withstand an adhesive tape test at least 50 times. After a 1500 time bending test, the resistance only increased by 5.2%. With laser-induced in situ synthesis, sintering, and simultaneous patterning of silver nanoparticles, this technology is promising for the facile fabrication of conducting electronic devices with flexible substrates [14] shown in Table 1.

Table 1 Typical and maximum module and cell conversion efficiencies at Standard Test Conditions.

Type	Typical module efficiency [%]	Maximum recorded module efficiency [%]	Maximum recorded laboratory efficiency [%]
Single crystalline silicon	12-15	22,7	24,7
Multicrystalline silicon	11-14	15,3	19,8
Amorphous silicon	5-7	-	12,7
Cadmium telluride	-	10.5	16.0
CIGS	-	12,1	18,2

With the rapid development of display-related markets, transparent conductive films (TCFs) with wide viewing angles, high transmittance, and low sheet resistance are in high demand. However, as a promising TCF material, metallic membranes with a sub-micrometer periodicity pattern fabricated by currently available techniques always reveal angle-dependent structural color, which can be a major issue in the development of wide-angle viewing display-related applications. Electrochromic devices based on the novel metallic film show more uniform color distribution than the devices based on metallic film with ordered single size apertures under indoor natural light irradiation. These findings demonstrate the applicability of the Au nanomesh film with dual size apertures in enhancing the display quality of high-performance optoelectronic devices [15].

Transparent conducting electrodes are essential components for numerous flexible optoelectronic devices, including touch screens and interactive electronics. Thin films of ITO—the prototypical transparent electrode material—demonstrate excellent electronic performances, but film brittleness, low infrared transmittance, and low abundance limit suitability for certain industrial applications.

Alternatives to ITO include conducting polymers, carbon nanotubes, and graphene. Although flexibility is greatly improved, the optoelectronic performance of these carbon-based materials is limited by low conductivity. Other examples include metal nanowire-based electrodes that can achieve a sheet resistance of less than $10 \Omega \text{ m}^{-1}$ at 90% transmission because of the high conductivity of the metals.

To achieve such great performance, metal nanowires must be defect-free, have conductivities close to their values in bulk, be as long as possible to minimize the number of wire-to-wire junctions, and exhibit small junction resistance. Here, we present a facile fabrication process that allows us to satisfy all these requirements and fabricate a new type of transparent conducting electrode that exhibits both superior optoelectronic performance (sheet resistance

of $\sim 2\Omega\text{ m}^{-1}$ at 90% transmission) and remarkable mechanical flexibility under both stretching and bending stresses.

The electrode is composed of a free-standing metallic nano trough network and is produced with a process involving electrospinning and metal deposition. We demonstrate the practical suitability of our transparent conducting electrode by fabricating a flexible touch-screen device and a transparent conducting tape [16]. Highly efficient photon recycling photosensitive optoelectronic device (POD) structures may include optical concentrating non-imaging collectors. Such device structures may be utilized with both organic and inorganic photoconverting heterostructures to enhance photoconversion efficiency. These photorecycling POD structures are particularly well suited for use with organic photoactive materials [17].

Carbon nanotube, Si, and Si-graphene -solar cells have attracted considerable interest recently owing to their potential in simplifying manufacturing process and lowering cost compared with Si cells. Until now, the power conversion efficiency of Si-graphene cells remains under 10% and well below that of the Si nanotube counterpart. Here, we involve a colloidal antireflection coating onto a monolayer Si-graphene solar cell and enhance the cell efficiency to 14.5% under standard illumination (air mass 1.5, 100 mW/cm²) with a stable antireflection effect over a long period.

The antireflection treatment was achieved by a simple spin-coating process, which significantly increased the short circuit current density and the incident photon-to-electron conversion efficiency to about 90% across the visible range. This result shows a great promise in developing high-efficiency Si-graphene solar cells in parallel to the more extensively studied carbon nanotube Si structures [18].

Singlet exciton fission, a process that generates two excitons from a single photon, is the most efficient of the various multiexciton generation processes studied to date offering the potential to increase the efficiency of solar devices. However, its unique characteristics splitting a photogenerated singlet exciton into two dark triplet states means that the empty absorption region between the singlet and triplet excitons must be filled by adding another material that captures low-energy photons. Thus, this phenomenon requires the development of specialized device architectures.

Pentacene-based PV devices typically show high external and internal quantum efficiencies. They have enabled researchers to characterize fission, including yield and the impact of competing loss processes, within functional devices. We review in situ probes of singlet fission that modulate the photocurrent using a magnetic field. We also summarize studies on the dissociation of triplet excitons into charge at the pentacene–buckyball (C₆₀) donor–acceptor interface. Multiple independent measurements confirmed that Pentacene triplet excitons can dissociate at the C₆₀ interface despite their relatively low energy.

Triplet excitons produced by singlet fission each have no more than half the energy of the original photo excitation; hence, they limit the potential open circuit voltage within a solar cell. Thus, if singlet fission increases the overall efficiency of a solar cell and not just doubles the photocurrent at the cost of halving the voltage, then photons in the absorption gap between the singlet and triplet energies of the singlet fission material should also be harvested. We review

two device architectures that attempt this process using long-wavelength materials: (1) a three-layer structure with long- and short-wavelength donors and an acceptor and (2) a simpler, two-layer combination of a singlet fission in tetracene with copper phthalocyanines inserted at the C₆₀ interface.

The bilayer approach included pentacene PV cells with an acceptor of infrared absorbing lead sulfide or lead selenide nanocrystals. Lead selenide nanocrystals are the most promising acceptors exhibiting efficient triplet exciton dissociation and high power conversion efficiency. Finally, we review architectures that use singlet fission materials to sensitize other absorbers, thereby effectively converting conventional donor materials to singlet fission dyes. In these devices, photo excitation occurs in a particular molecule and then energy is transferred to a singlet fission dye where the fission occurs. Rubrene inserted between a donor and an acceptor decouples the ability to perform singlet fission from other major PV properties, such as light absorption [19].

2.2 Fabrication of Organic and Hybrid Solar cells and their importance

Fullerene or phthalocyanine solar cells with an inverted structure were fabricated, and their PV properties, optical absorption, and microstructures were investigated. Silicon naphthalocyanine, gallium phthalocyanine, and poly (3-hexylthiophene) were used for donor materials, and 6, 6-phenyl C61-butyric acid methyl ester was also used as an acceptor material. Solar cells with an inverted structure provide higher conversion efficiencies by the addition of silicon naphthalocyanine and are more stable compared with solar cells with a normal structure in air. The nanostructures of the solar cells were investigated by transmission electron microscopy, and results showed the dispersion of nanocrystals in the active layers. The energy levels of the molecules were calculated, and a carrier transport mechanism was proposed [20]

The competition between exciton dissociation and charge transport in organic solar cells comprising poly (3-hexylthiophene) [P3HT] and phenyl-C61-butyric acid methyl ester [PCBM] was investigated by correlated scanning confocal photoluminescence and photocurrent microscopies. Contrary to the general expectation that higher photoluminescence quenching indicates higher photocurrent, microscale mapping of bulk heterojunction solar cell devices shows that photoluminescence quenching and photocurrent can be inversely proportional.

To understand this phenomenon, we constructed a model system by selectively laminating a PCBM layer onto a P3HT film to form a PCBM/P3HT planar junction on half of the device and a P3HT single junction on the other half. Upon thermal annealing to allow for inter diffusion of PCBM into P3HT, an inverse relationship between photoluminescence quenching and photocurrent was observed at the boundary between the PCBM/P3HT junction and the P3HT layer. Incorporation of PCBM in P3HT increased photoluminescence quenching, consistent with efficient charge separation, but conductive atomic force microscopic measurements revealed that PCBM decreased P3HT whole mobility, limiting the efficiency of charge transport. This result suggests that photoluminescence–quenching measurements should be used with caution in evaluating new organic materials for organic solar cells [21]. Example for the fabrications of organic solar cells and its method of Ultrasonic spray pyrolysis is shown in Fig 2(a-c)

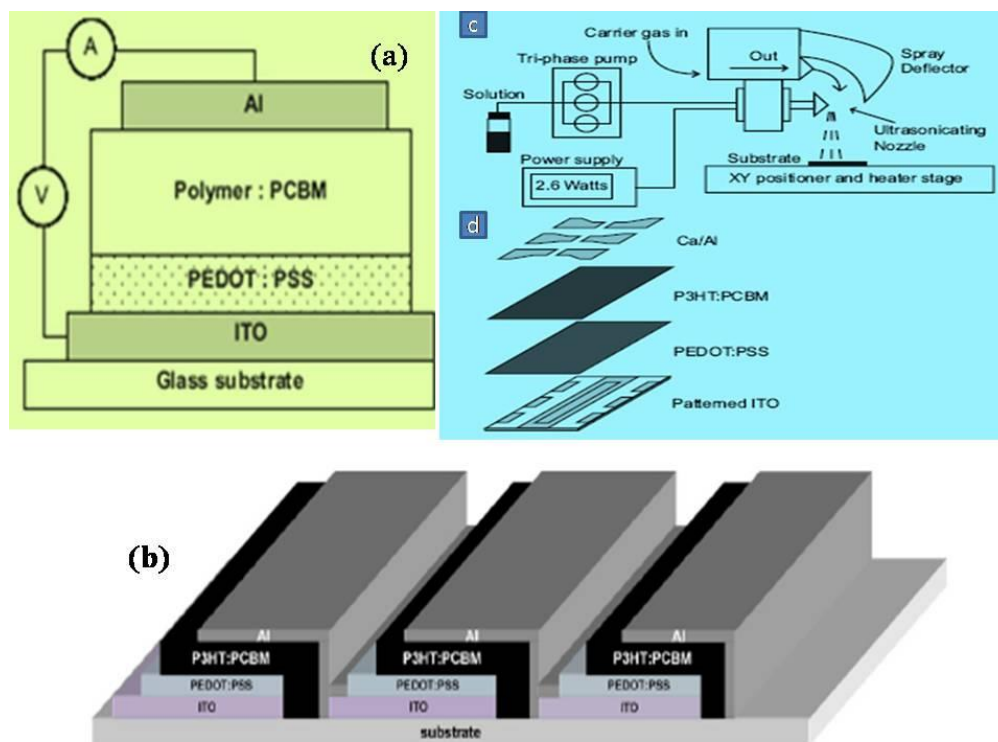


Figure 2 (a) Schematic of organic solar cell (b) Organic solar cells connected in series, (c) Ultrasonic spray pyrolysis.

The advantage of exciting single atoms with exponentially rising photons is a larger peak excitation probability within a narrower time interval.

Photonics combines many technologies, which explains its importance in many sectors. The Microphotonics & Nanophotonics track placed a spotlight on new manufacturing methods using laser technology, new components and micro-optical connections in data communications based on silicon photonics, and integrated optical microsystems for sensors.

Complementary metal-oxide semiconductor (CMOS) sensors acquire dynamic visual information in the form of a continuous stream of individual pixel data, sensing the context of a given scene rather than the entire data set. Professor Grätzel pioneered research in the field of energy and electron transfer reactions in mesoscopic systems and their use in energy conversion systems, particularly PV cells and photo-electrochemical devices for splitting water into hydrogen and oxygen, reducing carbon dioxide by sunlight, and storing electric power in lithium ion batteries. He discovered a new type of solar cell based on dye-sensitized nanocrystalline oxide films, which successfully mimic the light reaction occurring in green leaves and algae during natural photosynthesis.

Dye-sensitized solar cells (DSCCs) are produced industrially and sold commercially on the megawatt scale as lightweight flexible cells for powering portable electronic devices and as electricity-producing glass panels for application in building integrated PVs.

DSSCs have engendered perovskite solar cells that have revolutionized the whole field of PVs, reaching over 22% efficiency only a few years after their inception. This value exceeds the performance of silicon polycrystalline solar cells. Among the honorees in the “tech for a better world” category this time is Nano co Technologies, the UK-based developer of cadmium-free quantum dots for displays and lighting applications.

Divisive communication and value gaps separating the spheres of science and politics must be overcome if the UN’s global sustainable development goals are to be met.

“Photonics technologies have profound potential to help meet the UN’s sustainable development goals,” Arthurs said, citing solar and other renewable energy systems, water cleaning and desalination capabilities, energy-efficient lighting with LEDs, climate monitoring technologies, and fiber-optic communications as key examples.

Earlier in November, the Puerto Rico Photonics Institute based at the Universidad Metropolitana in San Juan organized the Photonics, Medicine, and Environment Symposium with speakers including Dean Bahaa Saleh of the College of Optics and Photonics at the University of Central Florida (CREOL) and Heidy Sierra from the Memorial Sloan-Kettering Cancer Center in New York.

The semiconductor devices that are used in optoelectronic and photonic applications often rely on strong excitonic resonances. These resonances can be tailored via bandgap engineering and electronic or photonic structuring.

To enable a more effective design of such devices, a complete understanding of light–matter interactions is highly desirable. Such understanding is likely to be of particular importance in the development of future quantum devices, for which a full knowledge of quantum states, their interactions, and coherence times is required. For example, the optical control of semiconductor coherences could play an integral role in quantum communications, computers, or simulators. In addition, inorganic nanostructures are model systems for the study of complex coherent mechanisms (e.g., photosynthesis [22] and photocatalytic devices [23])

2.3 Different types of dyes used and its advantages of dye sensitized solar cells

Over the last decade, coherent control of the optical response of semiconductor nanostructures and microcavities has uncovered the effects of structure and many-body Coulomb interactions. 2D coherent spectroscopy (2DCS) is a process in which the optical response is manipulated by using a sequence of laser pulses. The pulses spread the coherent signal into two spectral dimensions (typically absorption and emission frequencies). This approach enables the coherent response from single resonances and the coupling between resonances to be observed as separate spectral features. For example, confinement in quantum wells splits heavy- and light-hole excitons (due to their different effective masses), and 2DCS exhibits features that couple the two excitons [24–27]. Process of working electrodes of dye sensitized solar cell and its charge transfer were shown in Fig 3(a-c).

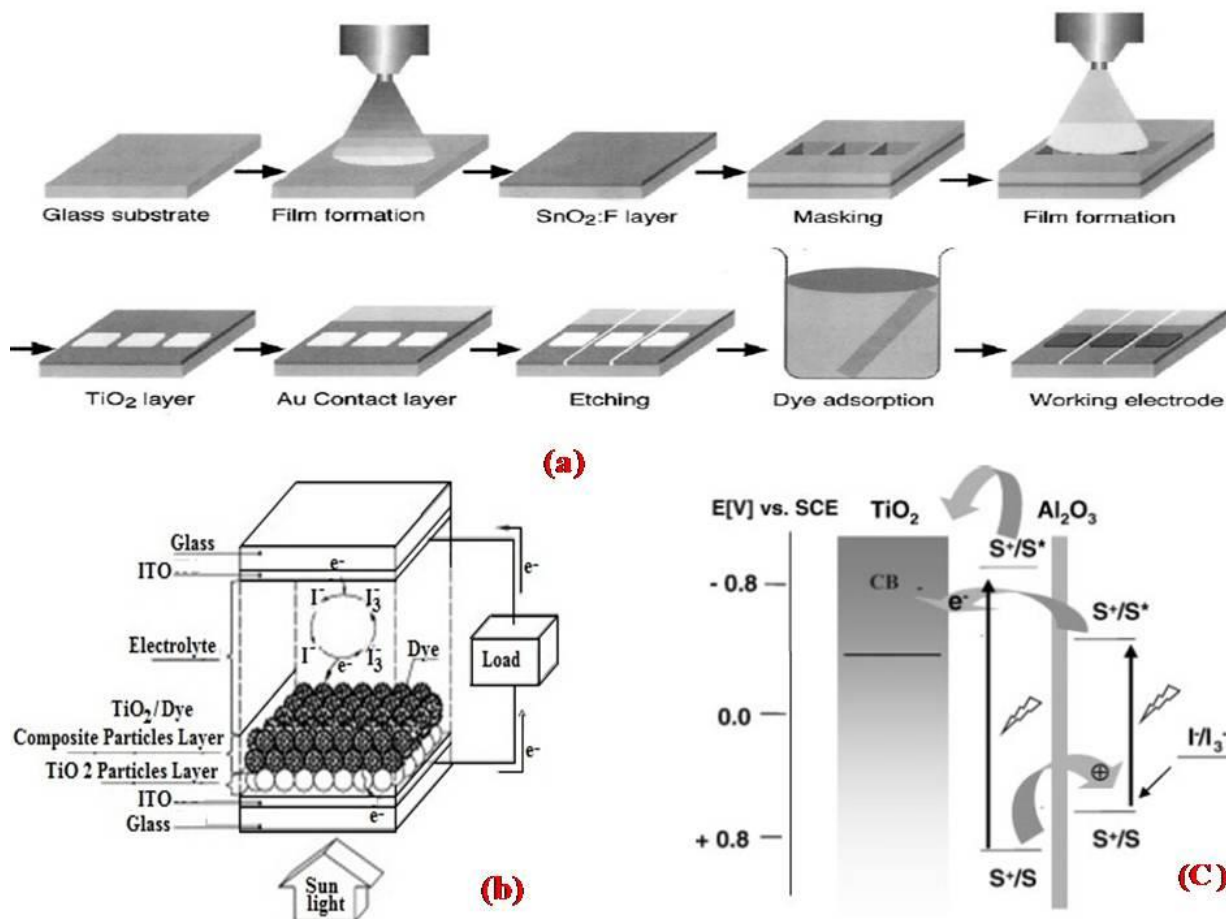


Figure 3 Process of producing working electrodes (b) Schematic of the dye sensitized solar cell with a sandwich TiO₂ thin film electrode and (c) Charge transfer process in multilayer co-sensitized nanocrystalline TiO₂ thin film.

However, spectral features may exhibit inhomogeneous broadening as a result of electronic confinement and can even yield information about a strain, as observed in bulk gallium arsenide (GaAs) [28]. Moreover, as a multi-pulse coherent-control scheme, 2DCS can also be used to examine non-radiative contributions (e.g., Raman or two-quantum coherence) by projecting these signals onto the emitted radiation. 2DCS has also been recently demonstrated as a powerful tool to examine photonic devices [29–31]. The success of this approach is, in part, due to the separation of various quantum mechanical excitation pathways and the sensitivity of the resulting spectral features to differing light–matter interactions.

A previous research used 2DCS to examine the coherent response of semiconductor microcavities [30]. To fabricate the microcavities, we precisely grew monolithic heterostructures of GaAs and related III-V semiconducting alloys. As illustrated in Figure 1, these structures comprise a narrow optical cavity (of GaAs) that is encased between two distributed Bragg mirrors (i.e., aluminum arsenide/GaAs bilayers) and contains an InGaAs (indium gallium arsenide) QW at the peak of the optical spatial mode. If the frequency of the optical cavity mode (γ) is in resonance with the excitonic mode of the QW (X), the system is

said to have zero detuning. Close to zero detuning, coupling of the cavity and exciton is sufficiently strong to result in normal-mode splitting.

Voltage-induced graphene oxide (GO) reduction is a facile and environmentally benign procedure for removing oxygen-containing functional groups from GO and recovering electrical conductivity. In this work, we perform a comprehensive investigation of the reduction process, structure, and electrical properties associated with voltage-reduced graphene oxide (V-rGO), obtained by applying a voltage between lateral electrode pairs. In situ optical microscopy during reduction reveals the growth of dendritic filaments of V-rGO that advance from the negative to positive terminal, eventually bridging and filling the entire electrode gap region. The growth rate of V-rGO filaments sharply increases with humidity and film thickness. Using varied electrode geometries, we demonstrate that V-rGO growth proceeds along electric field lines, opposite the field's direction. Following reduction, significant recovery of sp^2 carbon bonding and removal of oxygen-containing functional groups lead to electrical performance that is competitive with standard reduction schemes. Variable temperature resistance measurements identify Efros–Shklovskii variable-range hopping as the dominant transport mechanism, a result that is consistent with V-rGO acting as a polydisperse quantum dot array. Overall, this work suggests that voltage-induced reduction can be used in place of more cumbersome and hazardous reduction methods [35]. Localized voltage-induced reduction, initiated by a conductive atomic force microscope probe under ambient conditions, is used to pattern electrically conductive rGO regions in electrically insulating GO. This method reduces single- and multiple-layer GO on ultra-flat Au substrates with feature sizes as small as 4.0 nm, with the reduction resolution depending strongly on humidity and GO layer number.

In situ current levels during reduction are used to track reaction kinetics, which follow a rate-limited process where the generation and transport of hydrogen ions are the primary rate-limiting steps. Tip-enhanced Raman spectroscopy is used to map the nanoscale structure and local disorder in voltage-reduced GO and rGO single sheets. GO reduction decreases tip-enhanced Raman scattering intensity in both the D-band and G-band but does not affect the D/G intensity ratio, indicating that defects are not introduced by the reduction process [36]. Laminar composite electrodes are prepared for application in supercapacitors using a catalyzed vapor-phase polymerization (VPP) of 3,4-ethylenedioxythiophene (EDOT) on the surface of commercial carbon coated aluminum foil. These highly electrically conducting polymer films provide rapid and stable power storage per gram at room temperature. The chemical composition, surface morphology, and electrical properties are characterized by Raman spectroscopy, scanning electron microscopy, and conducting atomic force microscopy.

A series of electrical measurements including cyclic voltammetry, charge–discharge, and electrochemical impedance spectroscopy was also used to evaluate electrical performance. The processing temperature of VPP shows a significant effect on PEDOT morphology, the degree of orientation, and its electrical properties. The relatively high temperature increases the specific area and conductive domains of the PEDOT layer, which greatly benefit the capacitive behavior according to the data presented. Since the substrate is already highly conductive, the PEDOT-based composite can be used as an electrode material directly without adding a current collector. With this simple and efficient process, PEDOT-based composites exhibit a specific capacitance up to 134 F g^{-1} with the polymerization temperature of $110 \text{ }^\circ\text{C}$ [37-39]. Heliatek achieves 12% organic solar cell efficiency, Photonics.org, 23 January 2013. Inorganic materials such as electro-chemical solar cells using titanium dioxide in conjunction with an organic dye

and a liquid electrolyte already exceed 6% power conversion efficiencies and are about to enter the commercial market. Semiconducting polymers are also another interesting alternative to inorganic cells; these polymers combine the optoelectronic properties of conventional semiconductors with the excellent mechanical and processing properties of polymeric (i.e., plastic) materials [40,41]. The advantage of polymeric PV cells over electro-chemical cells is predominantly the absence of a liquid electrolyte, which generates problems with sealing against air, but also the prospect of even cheaper production using large-area devices and the application of flexible substrates.

Materials are the heart and soul of PV devices. PVs (solar cells) have been classified into various types according to the nature of materials. Device structure and nature of materials are critical for the overall efficiency and performance of PVs. However, in this particular review, we will be only converging on the nature of various materials used to develop solar cells and their performances. Solar cells are classified into different generations according to the nature and properties of materials [42].

2.4 Significance of few generations of Amorphous Silicon solar cells

First-generation solar cells developed in the midst of the 19th century were based purely on silicon-based materials [43]. First-generation PV cells are the dominant technology in the commercial production of solar cells, accounting for more than 86% of the solar cell market. Cells are synthesized using crystalline silica wafer consisting of a large-area single-layer p-n junction diode. Silicon is the most extensively used material in PV devices. Monocrystalline solar cells are first-generation PV materials that have long been available, indicating their robustness and endurance [44]. The monocrystalline silicon used in device fabrication with minimal defects and impurities can significantly affect the local electronic properties of monocrystalline silicon solar cell because of its outstanding electronic and optical properties that can reach up to 25% efficiency [45].

An effective solar cell needs (i) the absorption of a large portion of the incident solar radiation, (ii) the capable collection of both photogenerated electrons and holes, (iii) a junction with a built-in potential on the order of 1V, and (iv) a low internal series resistance [46]. The initial cost of producing monocrystalline silicon and its fragileness are the main disadvantages [47]. Polycrystalline silicon PV cell, polysilicon (p-Si), and multi-crystalline silicon (mc-Si) were commercialized in the early 1980s [48]. Disparate from monocrystalline solar cells, polycrystalline solar cells do not entail the Czochralski process [49]. For polycrystalline solar cells, raw silicon is melted and transferred into a square mold, which is cooled and cut into proper shaped wafers with the desired size. Unlike monocrystalline, polysilicon is comparatively cheap with minimal wastage of silicon during processing. The efficiency is lesser in polycrystalline solar cells (13%–16%) than monocrystalline cells because of impurities [50]. In addition, polysilicon materials are comparatively less heat resistant than other materials [51]. First to four generations and its one models are shown in Fig 4

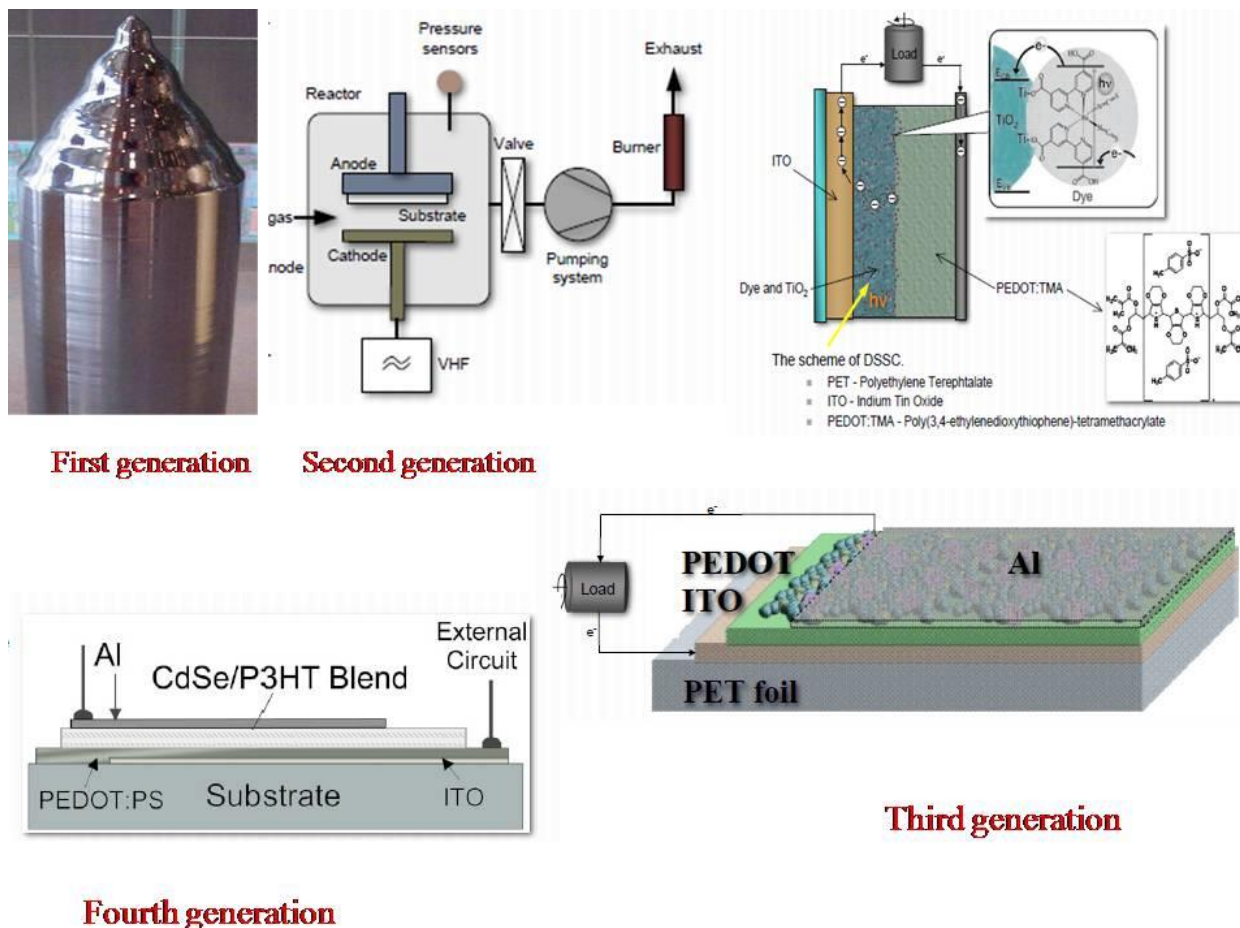


Figure 4 Various generation from First to Fourth of photovoltaic materials

Juwon Jeonga et al., in their work showed that Mesoporous TiO_2 particles can be effectively used as scattering particles in dye-sensitized solar cells(DSSCs), and since scattering particles are used to improve the light utilization of DSSCs, the approach used in their study could also be easily applied in other light harvesting devices such as water splitting device. [52]. O.L. Gribkova et al., investigated Poly(3,4-ethylenedioxythiophene) (PEDOT), films were electrodeposited in galvanostatic mode in the presence of salt or acid forms of sulfonated polyelectrolytes distinguished by different rigidity of the polymer main chain and presence of amid fragments in their structure [53]. Lian Jia et al., studied the performance of InGaAsP with Rapid thermal annealing (RTA) grown by molecular beam epitaxy with the bandgap energy of 1 eV [54].

Hongge Zheng et al., synthesize hexagonal formamidinium lead iodide $\text{CH}(\text{NH}_2)_2\text{PbI}_3$ (δ -FAPbI₃) perovskite nanorods which is an ideal candidate material for high performance photovoltaic and optoelectronic devices by a simple chemical solution method [55]. Tuo Zheng et al., studied the $\text{PbTi}_{1-x}\text{Fe}_x\text{O}_{3-\delta}$ (xPTFO) ferroelectric ceramics by means of structural characterizations, optical and magnetic measurements. All the samples show a tetragonal perovskite structure with uniform grains which is used to design optimal perovskite compounds for photovoltaic devices and magnetic storage [56]. Jun Lu et al., demonstrated an effective dc

reactive magnetron sputtering strategy and fabricated a well-aligned TiO₂ nanorod arrays for flexible dye-sensitized solar cells. PCE of 5.3% have been achieved by controlling the length of TiO₂ nanorod arrays [57] shown in Table 2.

Table 2 Various PV materials and its different applications.

Materials	Applications	References
Mesoporous TiO ₂ in dye-sensitized solar cells	Used in Dye sensitized solar cells	[52]
Poly(3,4-ethylenedioxythiophene) (PEDOT) Films	As a hole-transport (buffer) layer in organic photovoltaic cells	[53].
InGaAsP with Rapid thermal annealing (RTA)	As a dopant for PV materials that suffers from phase separation	[54].
Hexagonal formamidinium lead iodide CH(NH ₂) ₂ PbI ₃ (δ -FAPbI ₃) nanorods	Used in perovskite solar cells	[55].
PbTi _{1-x} Fe _x O _{3-δ} (xPTFO) ferroelectric ceramics	As optimal perovskite compounds for photovoltaic devices and magnetic storage	[56].
TiO ₂ nanorod arrays	As dye-sensitized solar cells	[57]
Cu ₂ FeSnSe ₄ (CFTSe) microparticles	As a absorption material for solar cell applications	[58]
Ferroelectric Pb(Zr,Ti)O ₃ (PZT) thin films and PbS quantumdots(QDs) -hybrid	Used in solution-processed quantum dots optoelectronics and solar cells	[59]
Poly (3-Hexylthiophene) (P3HT) thin films	Used in organic photovoltaic devices	[60]
C ₆₀ /DTDCTB/poly(3,4-ethylenedioxythiophene):poly(styrenesulfonate) (PEDOT:PSS)	As an efficient donor material in organic photovoltaics (OPVs)	[61]
GO@SnO ₂ /TiO ₂ nanofibers	Used in dye-sensitized solar cells (DSCs)	[62]

Jicheng Zhou et al., synthesized Cu₂FeSnSe₄ (CFTSe) microparticles by an atmospheric pressure liquid reflux method in triethylenetetramine and the CFTSe microparticles are found to have a single-phase stannite structure [58]. Young Hun Paik et al., presented a hybrid photovoltaic device based on PZT thin film with a PbS quantum dot layer using a solution based fabrication process. The overall power conversion efficiency was 0.75% which is higher when compared to PZT film only photovoltaic device [59] T. Sharma et al., investigated the modifications of Poly(3-Hexylthiophene) (P3HT) thin films by irradiating them with 90 MeV

Ni^{7+} ions at different fluencies (1×10^9 to 1×10^{11} ions/cm²) and it is found to have induced molecular ordering due to intense heating effect in the halo region of ion path [60].

Jisu Yoo et al., investigated the electronic structure of a narrow band gap small molecule ditolylaminothienyl–benzothiadiazole–dicyanovinylene (DTDCTB), possessing a donor-acceptor configuration, with regard to its application as an efficient donor material in organic photovoltaics (OPVs) [61]. Ibrahim M.A. Mohamed et al., synthesize the GO@SnO₂/TiO₂ nanofibers (NFs) by a facile method using electrospinning and hydrothermal processes. The photovoltaic performances showed that the efficiency of the device employed GO@SnO₂/TiO₂ photoanode gave 5.41%, which was higher than those of cells fabricated with SnO₂/TiO₂ NFs (3.41%) and GO@TiO₂ NFs (4.52%) photoanodes [62].

The gradients of zinc phthalocyanine/C60 were prepared by co-evaporation of the two materials from two sources to make a linear array of photodiode devices. ZnPc has a strong absorption in the mid- visible range, and photoinduced charge transfer between ZnPc and C60. It is also well as the substrate temperature, can significantly change the photovoltaic properties of the devices. ZnPc in C60 is easily done by co-evaporation of both molecules onto a surface from two separate sources at a distance; a gradient will be formed along the space extending in between the two evaporation sources. These structures are then used for evaluation of solar cell performance [63-72]. Dye-sensitized solar cells based on nanocrystalline TiO₂ electrodes are currently attracting widespread attention as a low cost alternative to conventional inorganic photovoltaic devices. Efficient light absorption for a monolayer of adsorbed sensitizer dye was achieved by the use of a mesoporous TiO₂ film structure [73-77] . This discussion were tabulated in Table 3.

Table 3 Different Materials and parameters of the various solar cells of workfunction, Fillfactor, PCE (%) and η (%).

Material	Work function	FF	PCE (%)	η (%)	
HEL		88.0		18.2	[63]
HEM		79.5		19.8	
Eurosil		83.6		24.4	
Wacker		83.6		24.4	[64]
PEDOT:PSS	5.25	0.68	9.93		
MoS ₂	5.0	0.67	9.53		
WS ₂	4.95	0.64	8.02		
GO	5.1	0.52	9.62		
CBL: Alq ₃ /Ca		0.48	-	2.28	[65]
PC ₆₀ :BM		0.67	3.44		[66]
C4:CFCMA		0.53	1.00		
BF-CBA		0.43	0.02		
C1-BFCBA		0.49	0.30		
C2-BFCBA		0.52	0.53		
C3-BFCBA		0.63	2.42		
C4-BFCBA		0.67	3.40		
C5-BFCBA		0.59	2.54		

C4-BFCTA		0.46	1.22		
TiO ₂		0.33		0.64	[67]
TiO ₂ +0.03% MWCNT		0.27		0.85	
TiO ₂ +0.06% MWCNT		0.31		0.78	
TiO ₂ +0.09% MWCNT		0.34		0.83	
TiO ₂ +0.15% MWCNT		0.32		0.37	
TiO ₂ +0.21% MWCNT		0.31		0.23	
ZnO/EY		56		1.60	[68]
ZnO/C		57		0.41	
ZnO/Rose		59		0.84	
ZnO/RhB		59		1.10	
ZnO/FGF		33		0.011	
ZnO/AO		49		0.024	
TiO ₂ /EY		43		0.03	
TiO ₂ /C		38		0.03	
TiO ₂ /RhB		57		0.60	
TiO ₂ /Rose		48		0.07	
TiO ₂ /FGF		47		0.04	
TiO ₂ /AO		40		0.013	
ZTO/EY		56		0.18	
ZTO/C		56		0.05	
ZTO/RhB		63		0.89	
ZTO/Rose		47		0.08	
ZTO/FGF		53		0.04	
ZTO/AO		21		0.002	
A(CB)		32.6	1.43±0.02		[69]
B(CB)		49.7	2.68±0.1		
C(CB)		51.4	2.51±0.2		
D(CB)		29.0	0.69±0.01		
E(CB)		38.4	0.09±0.01		
F(DCB)		53.04	2.67±0.02		
G(CB)		55.60	3.1±0.2		
H(DCB)		58.59	2.90±0.3		
I(DCB)		39.44	0.37±0.2		

J(DCB)		37.01	0.001		
Graphite	10.86±0.01	0.14±0.10	Graphite		[70]
RGO	12.29±0.01	0.26±0.20	RGO		
Carbon black	37.78±0.02	2.14±0.20			
Mixed	40.92±0.02	3.26±0.20			
Pt	56.76±0.02	4.52±0.25			
rGO	18	1.86			[71]
Crumpled Graphene	56	5.15			
PIDT-DTPQx	58.2		73%		[72]
PIDT-DTFPQx	61.7		64% (EQE)		
Dye- N719	0.66		8.67		[73]
G3	0.69		4.14		
G3	0.74		7.44		
G3	0.72		8.64		
G3	0.73		8.94		
G3	0.74		9.20		
G3	0.71		7.85		
G4	0.66		5.11		
G4	0.68		6.84		
G4	0.68		9.49		
G4	0.70		9.57		
G4	0.73		9.83		
G4	0.70		9.52		
G5	0.67		5.49		
G5	0.68		7.68		
G5	0.68		9.77		
G5	0.69		9.90		
G5	0.72		10.26		
G5	0.70		9.45		
P3HT:PCBM	0.39	1.24	25.64		[74]
Annealing time (min) 5	0.60	3.14	56.23		
30	0.62	3.51	58.76		
60	0.63	3.68	61.52		
120	0.65	4.05	64.16		
Polymer solar cell	0.68	5.0%	---		[75]
Perovskite:PU200 100:0	45.68±9.36		6.5±1.80		[76]

100:1	69.15±1.19		12.67±0.43		
100:3	54.49±5.90		8.63±1.45		
100:5	38.40		0.27		
PTB7	42	2.46 (2.34)			[77]
PTB7-DCB	47	4.22 (3.92)			
PTB7-Th	37	4.11 (3.91)			
PTB7-Th-DCB	49	6.07 (5.60)			

Polymer solar cells are becoming increasingly attractive because they show many potential advantages over traditional silicon-based solar cells. As an energy conservation device, efficiency is a very important parameter. In order to increase the PCE (Power Conversion Efficiency) of devices, some aspects should be taken into account, such as the absorption coefficients of the materials, the exciton dissociation rate, and the charge-carrier mobilities. Polymers with bandgaps above 2eV only absorb radiation in the ultraviolet (UV) and green part of the visible range. [78]. Conjugated polymers blended with soluble fullerene derivatives show a great potential for low cost, large area photovoltaics. One of the most promising devices following this approach are based on poly [2,6-(4,4-bis-(2-ethylhexyl)-4H-cyclopenta[2,1-b;3,4-b0]dithiophene)-alt-4,7-(2,1,3-benzothiadiazole)] (PCPDTBT), reaching power conversion efficiencies of up to 3.2% when combined with [6,6]-phenyl-C71-butyric acid methyl ester (PC70BM) [79]. Solar-energy generation, especially that of photovoltaics, has great potential as a renewable energy source because of its limitless and non-polluting properties. Recently, several research groups have reported that BHJ solar cells based on a composite film using poly(3-hexylthiophene) (P3HT) as an electron donor and [6,6]-phenyl-C61-butyric acid methyl ester (PCBM) as an electron acceptor show a power-conversion efficiency near 5%, which is the best reported performance for solution-processed polymer solar cells. In general, the performance of BHJ solar cells can be maximized by controlling the morphology of the active layer, because efficient photoinduced charge generation, transport, and collection at each electrode crucially depend on the nanometer-scale morphology of the composite films. [80]. Polymer electrolytes have reasonable ionic conductivities and eliminate the problems of sealing and solvent leakage.

3. CONCLUSIONS

Thermo chemical cycles characterized by the decomposition and regeneration of reactants present another avenue for hydrogen production. That materials used for the thermocycles are the main of this achievement. When the semiconductor is illuminated an electrical potential develops, potential can be enhanced by using specific materials of photovoltaic. Solar energy is not available at night, and the performance of solar power systems is affected by unpredictable weather patterns; therefore, storage media or back-up power systems must be used. Backup storage materials are also depending on photovoltaic devices. Tests on two solar-driven advanced oxidation processes, namely heterogeneous semiconductor photocatalysis and homogeneous photo-Fenton, both coupled to biological treatment, was carried out in order to identify the environmentally preferable alternative to treat industrial wastewaters containing non-biodegradable priority hazardous substances. Solar energy can be stored at high temperatures using molten salts. Salts are an effective storage medium because they are low-

cost, have a high specific heat capacity and can deliver heat at temperatures compatible with conventional power systems.

References

- [1]. T.M. Razykov, C.S. Ferekides, D. Morel, E. Stefanakos, H.S. Ullal, H.M. Upadhyaya, *Solar Energy* 85 (2011) 1580
- [2] N. Geetha, S. Sivaranjani, A. Ayeshamariam, Mariadhas Valan Arasu, N. Punithavelan, *Exp. Theo. NANOTECHNOLOGY* 2 (2018) 139
- [3]. T. Muneer, M. Asif & J. Kubie, *Energy Conversion and Management*, 44 (2003) 1
- [4]. T.M. Razykov, C.S. Ferekides, D. Morel, E. Stefanakos, H.S. Ullal, H.M. Upadhyaya, *Solar Energy* 85, (2011) 1580
- [5]. Mehra, S., Christoforo, M. G., Peumans, P., & Salleo, A. *Nanoscale*, 5(10), (2013), 4400
- [6]. Granqvist, C. G, *Solar energy materials. Advanced Materials*, 15(21), (2003)., 1789
- [7]. Gaynor, Whitney, Simone Hofmann, M. Greyson Christoforo, Christoph Sachse, Saahil Mehra, Alberto Salleo, Michael D. McGehee et al. " *Advanced Materials* 25, 29 (2013): 4006
- [8]. Mehra, Saahil, Mark G. Christoforo, Peter Peumans, and Alberto Salleo, *Nanoscale* 5,. 10 (2013): 4400
- [9]. Langley, D., Giusti, G., Mayousse, C., Celle, C., Bellet, D., & Simonato, J. P. *Nanotechnology*, 24(45), (2013), 452001
- [10]. Kim, Soo Jin, George Y. Margulis, Seung-Bum Rim, Mark L. Brongersma, Michael D. *Optics express* 21, 103 (2013): A305
- [11]. Jeng, Jun-Yuan, Yi-Fang Chiang, Mu-Huan Lee, Shin-Rung Peng, Tzung-Fang Guo, Peter Chen, and Ten-Chin Wen, *Advanced Materials* 25, 27 (2013): 3727
- [12]. Congreve, Daniel N., Jiye Lee, Nicholas J. Thompson, Eric Hontz, Shane R. Yost, Philip D. Reuswig, Matthias E. Bahlke, Sebastian Reineke, Troy Van Voorhis, and Marc A. Baldo. *Science* 340, 6130 (2013): 334
- [13]. Hong, Sukjoon, Junyeob Yeo, Gunho Kim, Dongkyu Kim, Habeom Lee, Jinhyeong Kwon, Hyungman Lee, Phillip Lee, and Seung Hwan Ko. *ACS nano* 7, 6 (2013) 5024
- [14]. Weiping Zhou, Shi Bai, Ying Ma, Delong Ma, Tingxiu Hou, Xiaomin Shi, and Anming Hu, *Applied Materials & Interfaces* 8 (37),(2016), 24887
- [15] Tengfei Qiu, Bin Luo, Fawad Ali, Esa Jaatinen, Lianzhou Wang, and Hongxia Wang, *ACS Appl. Mater. Interfaces*, 8 (35), 2016, 22768
- [16]. Wu, Hui, Desheng Kong, Zhichao Ruan, Po-Chun Hsu, Shuang Wang, Zongfu Yu, Thomas J. Carney, Liangbing Hu, Shanhui Fan, and Yi Cui., *Nature nanotechnology* 8 (2013) 421
- [17]. Forrest, Stephen R., Vladimir Bulovic, and Peter Peumans. U.S. Patent 6,333,458, issued December 25, (2001)
- [18]. Shi, E., Li, H., Yang, L., Zhang, L., Li, Z., Li, P., Shang, Y., Wu, S., Li, X., Wei, J. and Wang, K., *13*(4), (2013), 1776
- [19]. Lee, Jiye, Priya Jadhav, Philip D. Reuswig, Shane R. Yost, Nicholas J. Thompson, Daniel N. Congreve, Eric Hontz, Troy Van Voorhis, and Marc A. Baldo, *Accounts of chemical research* 46, 6 (2013): 1300
- [20]. Oku, T., Nose, S., Yoshida, K., Suzuki, A., Akiyama, T., & Yamasaki, Y. (2013). In *Journal of Physics: Conference Series*, 433, 012025, IOP Publishing.

- [21]. Oh, Soong Ju, Jongbok Kim, Jeffrey M. Mativetsky, Yueh-Lin Loo, and Cherie R. Kagan, *ACS Applied Materials & Interfaces* 8, 42 (2016), 28743
- [22]. G. D. Scholes, G. R. Fleming, A. Olaya-Castro, R. van Grondelle, *Nat. Chem.* 3 (2011) 763
- [23]. Cushing, Scott K., Jiangtian Li, Fanke Meng, Tess R. Senty, Savan Suri, Mingjia Zhi, Ming Li, Alan D. Bristow, and Nianqiang Wu. *Journal of the American Chemical Society* 134 (2012), 15033
- [24]. Nardin, Gaël, Travis M. Autry, Kevin L. Silverman, and Steven T. Cundiff, *Optics express* 21 (2013): 28617
- [25]. C. N. Borca, T. Zhang, X. Li, S. T. Cundiff, Optical two-dimensional Fourier transform spectroscopy of semiconductors, *Chem. Phys. Lett.* 416 (2005) 311
- [26]. M. Koch, J. Feldmann, G. von Plessen, E. O. Göbel, P. Thomas, K. Köhler, *Phys. Rev. Lett.* 69 (1992) 3631
- [27]. Bristow, Alan D., Tianhao Zhang, Mark E. Siemens, Steven T. Cundiff, and R. P. Mirin. *The Journal of Physical Chemistry B* 115, 18 (2011), 5365
- [28]. Glinka, Yuri D., Zheng Sun, Mikhail Erementchouk, Michael N. Leuenberger, Alan D. Bristow, Steven T. Cundiff, Allan S. Bracker, and Xiaoqin Li. *Physical Review B* 88,7 (2013), 075316
- [29]. Wilmer, Brian L., Daniel Webber, Joseph M. Ashley, Kimberley C. Hall, and Alan D. Bristow, *Physical Review B* 94 (2016) 075207
- [30]. Wen, Patrick, Gabriel Christmann, J. J. Baumberg, and Keith A. Nelson. *New Journal of Physics* 15 (2013) 025005
- [31]. Wilmer, Brian L., Felix Passmann, Michael Gehl, Galina Khitrova, and Alan D. Bristow, *Physical Review B* 91 (2015) 201304
- [32]. Takemura, N., Stephane Trebaol, M. D. Anderson, V. Kohnle, Yoan Léger, D. Y. Oberli, Marcia T. Portella-Oberli, and B. Deveaud, *Physical Review B* 92, 12 (2015), 125415
- [33]. Takemura, Naotomo, Stéphane Trebaol, Michiel Wouters, Marcia T. Portella-Oberli, and Benoît Deveaud, *Nature Physics* 10, 7 (2014), 500
- [34]. Moody, G., I. A. Akimov, H. Li, R. Singh, D. R. Yakovlev, G. Karczewski, M. Wiater, T. Wojtowicz, M. Bayer, and S. T. Cundiff, *Physical review letters* 112, 9 (2014), 097401
- [35]. Faucett, Austin C., Jaymes N. Flournoy, Jeremy S. Mehta, and Jeffrey M. Mativetsky. *Flat Chem* 1 (2016): 42
- [36]. Faucett, Austin C., and Jeffrey M. Mativetsky, *Carbon* 95 (2015): 1069
1. [37]. Tong, Linyue, Kenneth H. Skorenko, Austin C. Faucett, Steven M. Boyer, Jian Liu, Jeffrey M. Mativetsky, William E. Bernier, and Wayne E. Jones. *Journal of Power Sources* 297 (2015), 195
- [38]. Peumans, P., Yakimov, A. & Forrest, S. R. J. *Appl. Phys.* 93 (2003) 3693
- [39] T. S. Arun Samuel, M. Karthigai Pandian, A. Shenbagavalli, A. Arumugam, *Exp. Theo. NANOTECHNOLOGY* 2 (2018) 151
- [40]. B. O'Regan and M. Graetzel, *Nature* 353, (1991) 737
- [41]. Green, Martin A., Keith Emery, Yoshihiro Hishikawa, Wilhelm Warta, and Ewan D. Dunlop, *Progress in photovoltaics: research and applications* 23 (2015) 1
- [42] Ginley, David S., and Clark Bright. *Mrs Bulletin* 25 (2000) 15
- [43]. M. B. Armand, J. M. Chabagno, M. J. Duclot, North-Holland, Amsterdam, 131 (1979) 69
- [44]. W. A. Gazotti, G. Casalbore-Miceli, A. Geri, M.-A. De Paoli, *Adv. Mater.* 10 (1998) 60
- [45]. Weston, J. E., and B. C. H. Steele. *Solid State Ionics* 7 (1982) 75

- [46].Zhang, C.; Nguyen, T.; Sun, J.; Li, R.; Black, S.; Bonner, C.; Sun, S, *Macromolecules*, 42 (2009) 663
- [47] K. Tennakone, G. R. R. A. Kumara, K. G. U. Wijayantha, *Semicond. Sci.Technol.* 11 (1996) 1737
- [48]Tang, C. W. A two-layer organic solar cell. *Appl. Phys. Lett.* 48, (1986), 183–185
- [49] Shtein, M., Gossenberger, H. F., Benziger, J. B. & Forrest, S. R, *J. Appl. Phys.* 89 (2001) 1470
- [50]. P. D. Lund, “Impacts of energy storage in distribution grids with high penetration of photovoltaic power,” *Int. J. Distributed Energy Resources*, 3 (2007) 31
- [51]. Yu Z, Vlachopoulos N, Gorlov M, KlooL. Liquid electrolytes for dye-sensitized solar cells. *Dalton Trans* 40 (2011) 10289
- [52]. Juwon Jeonga, Woojeong Bakc, Jung-Woo Choia, Kyung Jae Leea, Jin Soo Kanga, Jin Kim, Dong Gwan Kim, Won Cheol Yoo, Yung-Eun Sung, *Electrochimica Acta* 222 (2016) 1079
- [53]. O.L. Gribkovaa, O.D. Iakobson, A. A. Nekrasov, V.A. Cabanova, V.A. Tverskoy, A.R. Tameev, A.V. Vannikov, *Electrochimica Acta*, 222 (2016) 409
- [54]. Lian Jia, Ming Tan, Chao Ding, Kazuki Honda, Ryo Harasawa, Yuya Yasue, Yuanyuan Wu, Pan Dai, Atsushi Tackeuchi, Lifeng Bian Shulong Lub, Hui Yang, *Journal of Crystal Growth* 458 (2017) 110
- [55]. Hongge Zheng, Jun Dai, *Materials Letters* 188 (2017) 232
- [56]. Tuo Zheng, Hongmei Deng, Wenliang Zhou, Pingxiong Yanga, Junhao Chu, *Materials Letters* 185 (2016) 380
- [57]. Jun Lu, Shaohong Xu, Yibo Du, Lin Lin, Yanli Wang, Dannong He, *Materials Letters* 188 (2017) 323
- [58]. Jicheng Zhou, YaoHu, XingChen, *Materials Letters*, 184 (2016) 216
- [59]. Young Hun Paik, Hossein Shokri Kojori, Ju-Hyung Yun, Sung Jin Kim, *Materials Letters*, 185 (2016) 247
- [60]. T. Sharma, R. Singhal, R. Vishnoi, G.B.V.S. Lakshmi, S. Chand, D.K. Avasthi, A.Kanjilal, S.K. Biswas, *Vacuum* 135 (2017) 73
- [61]. Jisu Yoo, Kwanwook Jung, Junkyeong Jeong, Gyeongho Hyun, Hyunbok Lee, Yeonjin Yi, *Applied Surface Science* 402 (2017) 41
- [62]. Ibrahim M.A. Mohamed, Van-Duong Dao, Ahmed S. Yasin, Ho-Suk Choi, KhalilAbdelrazek Khalil, Nasser A.M. Barakat, Nasser A.M. Barakat, Nasser A.M. Barakat, *Journal of Colloid and Interface Science* 490 (2017) 303
- [63] Zhao, Jianhua, Aihua Wang, Martin A. Green, and Francesca Ferrazza, *Applied Physics Letters* 73 (1998) 14
- [64]. Yu Geun Kim, Ki Chang Kwon, Quyet Van Le, Kootak Hong, Ho Won Jang and Soo Young Kim, *Journal of Power Sources* 319 (2016) 1
- [65] F. Martinez, Z. El Jouad, G. Neculqueo, L. Cattin, S. Dabos-Seignon, L. Pacheco, E. Lepleux P. Predeep, J. Manuvel, P. Thappily, M. Addou , J.C. Bern_ede, *Dyes and Pigments* 132 (2016) 185
- [66] Guangxin Liu, Tiantian Cao, Yijun Xia, Bo Song, Yi Zhou, Ning Chen, Yongfang Li, *Synthetic Metals* 215 (2016) 176
- [67] Umer Mehmood, Ibnel waleed A. Hussein, Khalil Harrabi, M.B.Mekki, Shakeel Ahmed, NouarTabet, *Solar Energy Materials & Solar Cells* 140 (2015) 174
- [68]. Mamta Rani, S.K.Tripathi, *Renewable and Sustainable Energy Reviews* 61 (2016) 97

- [69] M. Ikram, R. Murray, M. Imran, S. Ali, S. Ismat Shah, *Materials Research Bulletin* 75 (2016) 35
- [70] Ian. Y. Y. Bu, Ting Hao. Hu, *Solar energy*, 130 (2016) 81
- [71] Jae-Yup Kima,1, Jang Yeol Leea,1, Keun-Young Shina, Hansol Jeonga, Hae Jung Sona, Chul-Ho Lee, Jong Hyuk Park, Sang-Soo Leea, Jeong Gon Son, Min Jae Ko, *Applied Catalysis B: Environmental* 192 (2016) 342
- [72] Qunping Fan, Yu Liu, Huanxiang Jiang, Wenyan S, Linrui Duan, Hua Tan, Yuanyuan Li, *Organic Electronics* 33 (2016) 128
- [73] Roberto Grisorio, Luisa De Marco, Roberto Giannuzzi, Giuseppe Gigli, Gian Paolo Suranna, *Dyes and Pigments* 131 (2016) 282
- [74] By Jang Jo, Seok-In Na, Seok-Soon Kim, Tae-Woo Lee, Youngsu Chung, Seok-Ju Kang, Doojin Vak, and Dong-Yu Kim, *Advanced Functional Materials*, *Adv. Funct. Mater.* 19 (2009) 2398
- [75] W. Ma, C. Yang, X. Gong, K. Lee, A. J. Heeger, *Adv. Funct. Mater.* 15 (2005) 1617
- [76]. Pei-Yu Chuang, Ching-Nan Chuang, Chung-Chiang Yu, Lee-Yih Wang, Kuo-Hung Hsieh, *Polymer* 97 (2016) 196
- [77] Jea Woong Jo, Yujeong Kim, Min Jae Ko, Hae Jung Son, *Dyes and Pigments* 132 (2016) 103
- [78]. Dmitri Godovsky, Lichun Chen, Leif Pettersson, Olle Inganäs, Mats R. Andersson and Jan C. Hummelen, *Adv. Mater. Opt. Electron.* 10 (2000) 47
- [79]. Zhang, Fengling, Erik Perzon, Xiangjun Wang, Wendimagegn Mammo, Mats R. Andersson, and Olle Inganäs. *Advanced Functional Materials* 15 (2005) 745
- [80]. Lenés, Martijn, Mauro Morana, Christoph J. Brabec, and Paul WM Blom, *Advanced Functional Materials* 19 (2009) 1106

© 2019 The Authors. Published by IFIA (<https://etn.iraqi-forum2014.com/>). This article is an open access article distributed under the terms and conditions of the Creative Commons Attribution license (<http://creativecommons.org/licenses/by/4.0/>).